Cumhuriyet Science Journal
e-ISSN: 2587-246X
ISSN: 2587-2680
Cumhuriyet Sci. J., 42(2) (2021) 372-379
http://dx.doi.org/10.17776/csj.796263

Numerical solutions of the randall-wilkins and one trap one recombination models for first order kinetic

Erdem UZUN [1,*]

[1] *Karamanoğlu Mehmetbey University, Department of Physics, 70200, Karaman / TURKEY*

Abstract

Randall-Wilkins and One Trap One Recombination (otor) models have been proposed to explain thermoluminescence emission and it should be emphasized that each model has its own allowed charge carrier transitions, trapping parameters and differential equations set. The equations are generally first or higher order linear differential equations with constant coefficients and their numerical solutions are an initial value problem. From this point on, numerical solutions of the thermoluminescence equations have been effectively used. In this paper the models were solved, numerically by using Euler and Runge-Kutta methods on Mathematica 8.0. In this work, although the fastest result calculated by Explicit Euler method, the most accurate results were calculated Linearly Implicit Euler method.

Article info

History:
Received: 17.10.2020
Accepted: 18.03.2021

Keywords:
Thermoluminescence,
Simulation
Euler, Runge-Kutta,
Otor.

1. Introduction

Although differential equations proposed by thermoluminescence (TL) models are relatively basic, their analytic solutions are not possible. One of the ways to overcome the difficulty is to simplify the equations under various assumptions and the another is to perform numerical solutions. Numerical solutions of the TL equations are widely used in TL applications [1,2]. Pros and cons arguments of the numerical solutions of the TL equations were argued by McKeever[3] and many others[1,4]. The first numerical approximation of the TL equations was performed by Kemmey et al[5] but exact numerical solutions were given by Kelly et al[6] for the first time. Moreover, Shenker and Chen[7], Chen et al[8] and many others have published numerical solutions of the TL equations up to now.

In this paper we discuss numerical solutions of the Randall-Wilkins and otor models by using different numerical methods such as Euler's and Runge-Kutta methods. All solutions are performed in Mathematica 8.0.

2. Randall and Wilkins Model

The simplest model of TL emission is proposed by Randall and Wilkins and it consists of an electron trap level (N), and a recombination center[9,10]. Randall and Wilkins assumed that recombination rate of the free charge carrier is significantly faster than re-trapping and thus, TL emission can be given as Eq.1. Energy band diagram and allowed transitions are given in Fig. Figure **1**.

$$I_{TL} = n.s.\exp\left\{-\frac{E_e}{k.T}\right\} \tag{1}$$

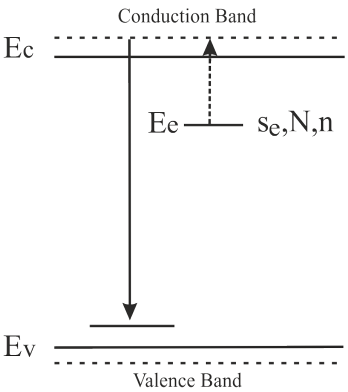

Figure 1. Schematic energy level diagram of Randall-Wilkins model

Here, N is trapping states (in cm^{-3}) and with instantaneous occupancy n. The activation energy for the electron trap is E_e (in eV) and the frequency factor is s_e (s^{-1}). k is the Boltzmann constant ($k = 8.617\times10^{-5}$ eV K^{-1})

3. OTOR Model

OTOR model consists of an electron trap level, and a recombination center (Fig.Figure **2**), but there are three allowed transitions are available; trapped electrons can

*Corresponding author. *e-mail address: erdemuzun@kmu.edu.tr* be released by thermally; free electrons are trapped by N or recombined in center[11,12]. Differential equations representing the charge carrier traffic as a function of temperature and time are given:

$$\frac{dn_c}{dt} = n.s_e.\exp\left\{-\frac{E_e}{k.T}\right\} - n_c\left(N-n\right)A_{te} - n_c.\left(n+n_c\right).A_{re} \quad (2)$$

$$\frac{dn}{dt} = n_c.\left(N-n\right)A_{te} - n.s_e.\exp\left\{-\frac{E_e}{k.T}\right\} \quad (3)$$

$$I_{TL} = -\eta.n_c.\left(n+n_c\right).A_{re} \quad (4)$$

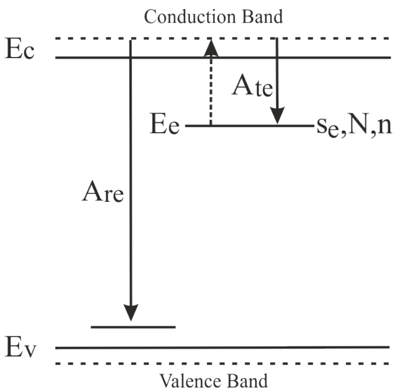

Figure 2 Schematic energy level diagram of OTOR model

Here, A_{te} and A_{re} are re-trapping and recombination probability coefficients. Moreover, if A_{re}=1 and A_{te}=0 are taken, OTOR model transforms into Randall and Wilkins model.

3.1. Experimental methods

Samples used in this study is α-Al_2O_3 powder. α-Al_2O_3 has four glow peaks[13,14] (Figure Figure **1**) and the first peak is located at 117±2°C. The first peak has first ordered kinetic and it is used for the comparisons of the simulations. In order to isolate of the first peak, some experimental procedures are performed. Firstly, α-Al_2O_3 sample is annealed at 600°C for 15 min to erase any residual radiation effects. Then, it is spread on thin aluminum disk about 10mg and it is irradiated at room temperature using the beta rays from a calibrated ^{90}Sr–^{90}Y source. Glow curve of the sample is recorded between 40-400°C temperature ranges using linear heating rate as reference. Thereafter, the annealing and irradiation procedure repeated and the sample is heated up to T_s and cooled to room temperature. Lastly, glow curve of the sample is recorded between 40-400°C temperature ranges. Last glow curve is subtracted from the first one and the peak is obtained in isolated manner. The procedures are repeated several times for different T_s and T_s's are chosen between 100°C-140°C. After then trap parameters are calculated by using peak shape[4,15,16], various heating rate[4,17] and initial rise[4,18] methods. Moreover, initial trap occupancy was also measured by using area under the glow curve. Results are given in Table Table **1** and Figure Figure **4**.

Table 1. Experimental trap parameters

	E_e (eV)	S_e (s^{-1})	b	n_o(cm^3 s^{-1})
FOK peak	0.89±0.02	2.17±0.07×10^{10}	1.00	1.18×10^5

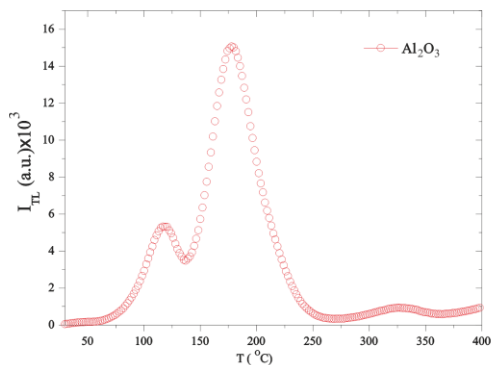

Figure 3. Thermoluminescence glow curve of the α-Al_2O_3

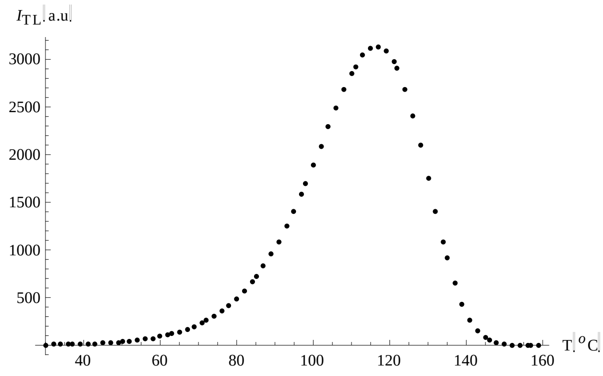

Figure 4. First peak of the α- Al_2O_3 used in this study

4. Numerical Analysis

In this study, all numerical solutions are calculated iteratively. Each solution is started from a given initial particular value of I_{TL} (n_o, n_{co}) at T_{min}, and then takes a sequence of steps, trying eventually to cover the whole range T_{min} to T_{max}. Experimental trap parameters (Table 1) are taken as initial conditions and other parameters such as A_{re}, A_{te} et al are chosen realistically but in a broad range. Numerical solutions of the equations are performed using Explicit Euler[19,20], Generalized Euler[19], Classical Runge-Kutta[21], and Implicit Runge–Kutta methods [21–23]. The techniques are summarized in Figure Figure 5. Simulations of the models are performed on Mathematica 8.0[24,25].

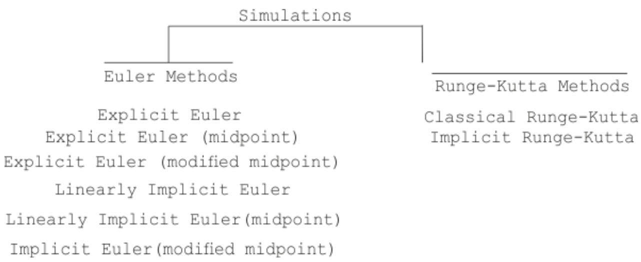

Figure 5. Numerical methods and sub methods used in this study

5. Results and Discussions

Numerical solutions of the models are performed for different step sizes and differential orders. In order to make comparison easier, figure of merit[26] (FOM) and step sizes are drawn together. All the simulations were performed by using experimentally measured trap parameters from Table Table **1**. It is important to point out that that although the numerical solutions of the TL models are successful in explaining some TL behaviors of the materials theoretically, they do not match the results of the experiments. However, Uzun[27–30] and many others[3,8,11] shown that the simulations are in good agreement with experiment only when the simulation is started with the assumption of n_o=N. Thus, N=1.20×10^{5}cm^{3}s^{-1} was taken in all the simulations.

Randall-Wilkins and OTOR models were solved numerically by using Explicit Euler, Explicit Euler (midpoint), Explicit Euler (modified midpoint), Linearly Implicit Euler, Linearly Implicit Euler (midpoint), Implicit Euler (modified midpoint), Classical Runge-Kutta and Implicit Runge-Kutta.

Randall-Wilkins model was solved numerically by using Explicit Euler methods and results are given in Table **2**. Although the Euler methods can simulate the Randall-Wilkins model by wide range of steps (10^{-1}-10^{-4}), the methods can be solved the OTOR model for a restricted step range (step size≤2.0×10^{-5}).

Table 2. Simulation results of the Explicit Euler

It. Nu.	St. Sz.	FOM	It. Nu.	St. Sz.	FOM
fok			otor		
1.59×10^3	10^{-1}	0.45(5266)	3.18×10^7	0.5×10^{-5}	0.29(0760)
1.59×10^4	10^{-2}	0.30(5387)	1.59×10^7	1.0×10^{-5}	0.29(0767)
1.59×10^5	10^{-3}	0.29(2113)	1.06×10^7	1.5×10^{-5}	0.29(0776)
1.59×10^6	10^{-4}	0.29(0889)	7.95×10^7	2.0×10^{-5}	0.29(0781)

Table 3. Simulation results of the Explicit Euler (midpoint)

It. Nu.	St. Sz.	FOM	It. Nu.	St. Sz.	FOM
fok			otor		
2.03×10^5	10-1	0.29(0753912)	1.30×10^7	0.5×10^{-5}	0.29(0760)
2.03×10^5	10^{-2}	0.29(0753989)	1.30×10^7	1.0×10^{-5}	0.29(0767)
2.03×10^5	10^{-3}	0.29(0753945)	1.30×10^7	1.5×10^{-5}	0.29(0776)
2.03×10^5	10^{-4}	0.29(0754040)	1.30×10^7	2.0×10^{-5}	0.29(0781)

Table 4. Simulation results of the Explicit Euler (modified midpoint)

It. Nu.	St. Sz.	FOM	It. Nu.	St. Sz.	FOM
fok			otor		
3.05×10^5	10-1	0.29(0753)	1.19×10^7	0.5×10^{-5}	0.29(0754)
3.05×10^5	10^{-2}	0.29(0753)	1.21×10^7	1.0×10^{-5}	0.29(0754)
3.05×10^5	10^{-3}	0.29(0753)	1.16×10^7	1.5×10^{-5}	0.29(0754)
3.05×10^5	10^{-4}	0.29(0753)	1.17×10^7	2.0×10^{-5}	0.29(0754)

Table 5. Simulation results of the Linearly Implicit Euler

It. Nu.	St. Sz.	FOM	It. Nu.	St. Sz.	FOM
fok			otor		
3.18×10^4	10^{-1}	0.24(6577)	6.36×10^7	0.5×10^{-5}	0.29(0747)
3.18×10^5	10^{-2}	0.27(8494)	3.18×10^7	1.0×10^{-5}	0.29(0740)
3.18×10^6	10^{-3}	0.28(9486)	2.12×10^7	1.5×10^{-5}	0.29(0731)
3.18×10^7	10^{-4}	0.29(0618)	1.59×10^7	2.0×10^{-5}	0.29(0726)

Table 6. Simulation results of the Linearly Implicit Euler (midpoint)

It. Nu.	St. Sz.	FOM	It. Nu.	St. Sz.	FOM
fok			otor		
1.44×10^5	10^{-1}	0.29(0801)	5.75×10^6	0.5×10^{-5}	0.29(0767)
1.44×10^5	10^{-2}	0.29(0802)	5.75×10^6	1.0×10^{-5}	0.29(0759)
1.44×10^5	10^{-3}	0.29(0829)	5.75×10^6	1.5×10^{-5}	0.29(0764)
1.44×10^5	10^{-4}	0.29(0816)	5.75×10^6	2.0×10^{-5}	0.29(0760)

Table 7. Simulation results of the Linearly Implicit Euler (modified midpoint)

It. Nu.	St. Sz.	FOM	It. Nu.	St. Sz.	FOM
fok			otor		
1.92×10^5	10^{-1}	0.29(0769)	9.05×10^6	0.5×10^{-5}	0.29(1068)
1.92×10^5	10^{-2}	0.29(0586)	9.05×10^6	1.0×10^{-5}	0.29(1187)
1.92×10^5	10^{-3}	0.29(0846)	9.05×10^6	1.5×10^{-5}	0.29(1158)
1.92×10^5	10^{-4}	0.29(0633)	9.05×10^6	2.0×10^{-5}	0.29(1068)

Table 8. Simulation results of the Classical Runge-Kutta

Diff. Ord.	It. Nu.	St. Sz.	FOM	It. Nu.	St. Sz.	FOM
	fok			otor		
3	6.36×10^{3}	10^{-1}	0.29(0754)	1.27×10^{8}	0.5×10^{-5}	0.29(0754)
	6.36×10^{4}	10^{-2}	0.29(0754)	6.36×10^{7}	1.0×10^{-5}	0.29(0754)
	6.36×10^{5}	10^{-3}	0.29(0754)	4.24×10^{7}	1.5×10^{-5}	0.29(0754)
	6.36×10^{6}	10^{-4}	0.29(0754)	3.18×10^{7}	2.0×10^{-5}	0.29(0754)
4	7.65×10^{3}	10^{-1}	0.29(0754)	-		
	7.65×10^{4}	10^{-2}	0.29(0754)			
	7.65×10^{5}	10^{-3}	0.29(0754)			
	7.65×10^{6}	10^{-4}	0.29(0754)			
5	6.36×10^{3}	10^{-1}	0.29(0754)	-		
	6.36×10^{4}	10^{-2}	0.29(0754)			
	6.36×10^{5}	10^{-3}	0.29(0754)			
	6.36×10^{6}	10^{-4}	0.29(0754)			
6	6.36×10^{3}	10^{-1}	0.29(0754)	-		
	6.36×10^{4}	10^{-2}	0.29(0754)			
	6.36×10^{5}	10^{-3}	0.29(0754)			
	6.36×10^{6}	10^{-4}	0.29(0754)			
7	6.36×10^{3}	10^{-1}	0.29(0754)	-		
	6.36×10^{4}	10^{-2}	0.29(0754)			
	6.36×10^{5}	10^{-3}	0.29(0754)			
	6.36×10^{6}	10^{-4}	0.29(0754)			
8	6.36×10^{3}	10^{-1}	0.29(0754)	-		
	6.36×10^{4}	10^{-2}	0.29(0754)			
	6.36×10^{5}	10^{-3}	0.29(0754)			
	6.36×10^{6}	10^{-4}	0.29(0754)			
9	6.36×10^{3}	10^{-1}	0.29(0754)	-		
	6.36×10^{4}	10^{-2}	0.29(0754)			
	6.36×10^{5}	10^{-3}	0.29(0754)			
	6.36×10^{6}	10^{-4}	0.29(0754)			

Table 9. Simulation results of the Implicit Runge-Kutta

Diff. Ord.	It. Nu.	St. Sz.	FOM	It. Nu.	St. Sz.	FOM
	fok			otor		
3	8.06×10^{3}	10^{-1}	0.29(0754)	9.14×10^{3}	10^{-1}	0.29(0754)
	7.94×10^{4}	10^{-2}	0.29(0754)	7.95×10^{4}	10^{-2}	0.29(0754)
	6.63×10^{5}	10^{-3}	0.29(0754)	7.26×10^{5}	10^{-3}	0.29(0754)
	4.77×10^{6}	10^{-4}	0.29(0754)	5.58×10^{6}	10^{-4}	0.29(0754)
4	9.36×10^{3}	10^{-1}	0.29(0754)	1.04×10^{4}	10^{-1}	0.29(0754)
	9.23×10^{4}	10^{-2}	0.29(0754)	9.24×10^{4}	10^{-2}	0.29(0754)
	7.92×10^{5}	10^{-3}	0.29(0754)	8.55×10^{5}	10^{-3}	0.29(0754)
	6.06×10^{6}	10^{-4}	0.29(0754)	6.87×10^{6}	10^{-4}	0.29(0754)
5	1.50×10^{4}	10^{-1}	0.29(0754)	1.70×10^{4}	10^{-1}	0.29(0754)
	1.09×10^{5}	10^{-2}	0.29(0754)	1.46×10^{5}	10^{-2}	0.29(0754)
	1.02×10^{6}	10^{-3}	0.29(0754)	1.27×10^{6}	10^{-3}	0.29(0754)
	1.02×10^{7}	10^{-4}	0.29(0754)	1.16×10^{7}	10^{-4}	0.29(0754)
6	1.89×10^{4}	10^{-1}	0.29(0754)	2.09×10^{4}	10^{-1}	0.29(0754)
	1.48×10^{5}	10^{-2}	0.29(0754)	1.85×10^{5}	10^{-2}	0.29(0754)
	1.41×10^{6}	10^{-3}	0.29(0754)	1.66×10^{6}	10^{-3}	0.29(0754)
	1.41×10^{7}	10^{-4}	0.29(0754)	1.54×10^{7}	10^{-4}	0.29(0754)
7	2.29×10^{4}	10^{-1}	0.29(0754)	3.02×10^{4}	10^{-1}	0.29(0754)
	2.08×10^{5}	10^{-2}	0.29(0754)	2.64×10^{5}	10^{-2}	0.29(0754)
	2.08×10^{6}	10^{-3}	0.29(0754)	2.43×10^{6}	10^{-3}	0.29(0754)
	2.08×10^{7}	10^{-4}	0.29(0754)	2.28×10^{7}	10^{-4}	0.29(0754)
8	2.94×10^{4}	10^{-1}	0.29(0754)	3.66×10^{4}	10^{-1}	0.29(0754)
	2.73×10^{5}	10^{-2}	0.29(0754)	3.29×10^{5}	10^{-2}	0.29(0754)
	2.73×10^{5}	10^{-3}	0.29(0754)	3.07×10^{6}	10^{-3}	0.29(0754)
	2.73×10^{7}	10^{-4}	0.29(0754)	2.92×10^{7}	10^{-4}	0.29(0754)
9	3.66×10^{4}	10^{-1}	0.29(0754)	4.85×10^{4}	10^{-1}	0.29(0754)
	3.66×10^{5}	10^{-2}	0.29(07549	4.37×10^{5}	10^{-2}	0.29(07549
	3.66×10^{6}	10^{-3}	0.29(0754)	4.10×10^{6}	10^{-3}	0.29(0754)
	3.66×10^{7}	10^{-4}	0.29(0754)	3.91×10^{7}	10^{-4}	0.29(0754)

Conclusions

In this paper Randall-Wilkins and One Trap One Recombination models were solved, numerically by using Mathematica for Euler and Runge-Kutta methods. In order to comparison of the simulations, some experiments were also performed. Fundamental trap parameters were measured, experimentally and used as initial conditions. each simulation was compared by the experiments and FOM was calculated. The fastest results were calculated by Linear Euler method but, the most accurate results were calculated by Linearly Implicit Euler method. In the application, not only precision but also machine time is important and here Linearly Implicit Euler method is suggested by the authors.

Acknowledge

This work has been funded by Karamanoğlu Mehmetbey University Commission of Scientific Research Projects (Project Number: 20-M-16).

Conflicts of interest

The authors state that did not have conflict of interests.

References

[1] Chen R., Pagonis V., Thermally and Optically Stimulated Luminescence: A Simulation Approach. 1st ed. Wilthshire, (2011) 245-272.

[2] Pagonis V., Kitis G., Furetta C., Numerical and Practical Exercises in Thermoluminescence. 1st ed. New York, (2006) 1-21.

[3] McKeever S. W. S., Thermoluminescence of Solids. 1st ed. Cambridge, (1985) 20-198.

[4] Chen R., McKeever S. W. S., Theory of Thermoluminescence and Related Phenomena. 1st ed. Singapore, (1997) 17-205.

[5] Kemmey P. J., Townsend P. D. Levy, P. W., Numerical Analysis of Charge-Redistribution Processes Involving Trapping Centers, *Phys. Rev.*, 155 (1967) 917–920.

[6] Kelly P., Laubitz M. J., Bräunlich P., Exact Solutions of the Kinetic Equations Governing Thermally Stimulated Luminescence and Conductivity, *Phys. Rev. B.*, 4 (1971) 1960–1968.

[7] Shenker D., Chen R., Numerical Solution of the Glow Curve Differential Equations, *J. Comput. Phys.*, 10 (1972) 272–283.

[8] Chen R., Hornyak W. F., Mathur V. K., Competition Between Excitation and Bleaching of Thermoluminescence, *J. Phys. D. Appl. Phys.*, 23 (1990) 724–728.

[9] Randall J. T., Wilkins M. H. F., Phosphorescence and Electron Traps - I. The Study of Trap Distributions, *Proc. R. Soc. London. Ser. A. Math. Phys. Sci.*, 184 (1945) 365–389.

[10] Randall J. T., Wilkins M. H. F., Phosphorescence and Electron Traps II. The Interpretation of Long-Period Phosphorescence, *Proc. R. Soc. London. Ser. A. Math. Phys. Sci.*, 184 (1945) 390–407.

[11] McKeever S. W. S., Chen R., Luminescence Models, *Radiat. Meas.*, 27 (1997) 625–661.

[12] Bos A. J. J., Theory of Thermoluminescence, *Radiat. Meas.*, 41 (2006) 45–56.

[13] Uzun E., Characterization of Thermoluminescent Properties of Seydisehir Alumina and Investigation of Properties of Dose Response, PD, Yıldız Technical University, Science and Engineering, 2008.

[14] Uzun E., Yarar Y., Yazıcı A. N., Electron Immigration From Shallow Traps to Deep Traps by Tunnel Mechanism on Seydiehir Aluminas, *J. Lumin.*, 131 (2011) 2625–2629.

[15] Kitis G., Pagonis V., Peak Shape Methods for General Order Thermoluminescence Glow-Peaks: A Reappraisal, *Nucl. Instruments Methods Phys. Res. Sect. B Beam Interact. with Mater. Atoms.*, 262 (2007) 313–322.

[16] Sunta C. M., Feria A. W. E., Piters T. M., Watanabe S., Limitation of Peak Fitting and Peak Shape Methods for Determination of Activation Energy of Thermoluminescence Glow Peaks, *Radiat. Meas.*, 30 (1999) 197–201.

[17] Chen R., Winer S. A. A., Effects of Various Heating Rates on Glow Curves, *J. Appl. Phys.*, 41 (1970) 5227–5232.

[18] Chen R., Methods for Kinetic Analysis of Thermally Stimulated Processes, *J. Mater. Sci.*, 11 (1976) 1521–1541.

[19] Stoer J., Bulirsch R., Introduction to Numerical Analysis, 3rd ed. New York, (2002) 471-480.

[20] Hoffman J. D., Numerical Methods for Engineers and Scientists, 2nd ed. West Lafayette, (2015) 352-414.

[21] Conte S. D. D., de Boor C., The Solution of Differential Equations. In: Conte S. D. D., de Boor C., (Eds). Elementary Numerical Analysis: An Algorithmic Approach, 1st ed. Philadelphia: Siam, (2017) 346-405.

[22] Shampine L. F., Some practical Runge-Kutta formulas, *Math. Comput.*, 46 (1986) 135–135.

[23] Dormand J. R., Prince P. J., Runge-Kutta triples, *Comput. Math. with Appl.*, 12 (1986) 1007–1017.

[24] Nearing J., Mathematical Tools for Physics, 1st ed. Miami, (2010) 320-350.

[25] Sofroniou M., Knapp R., Advanced Numerical Differential Equation Solving in Mathematica, 1st ed. Online, (2008) 17-162.

[26] Balian H. G., Eddy N. W., Figure-of-merit (FOM), an improved criterion over the normalized chi-squared test for assessing goodness-of-fit of gamma-ray spectral peaks, *Nucl. Instruments Methods*, 145 (1977) 389–395.

[27] Uzun E., Theoretical Modeling and Numerical Solutions of the Some Standard Thermoluminescence Detector Crystals, *Turkish J. Phys.*, 37 (2013) 304–311.

[28] Uzun E., On the Numerical Solution of the One Trap One Recombination Model for First Order Kinetic, *AASCIT J. Phys.*, 3(5) 2017 36-43.

[29] Uzun E., Korkmaz M. E., Numerical Solutions of Schön-Klasens Model for Luminescence Efficiency, *EPJ Web Conf.*, 100 (2015) 04005p1-p3.

[30] Uzun E., Discussions on the Numerical Solutions of Schön-Klasens Model: Charge Carrier Traps Depth, *Sigma J. Eng. Nat. Sci.*, 33 (2015) 421–426.